

Contact Resistance of Flexible, Transparent Carbon Nanotube Films with Metals

Hua Xu, Lei Chen and Nikolai Zhitenev

Center for Nanoscale Center for Nanoscale Science and Technology, National Institute of Standards and Technology, Gaithersburg, Maryland 20899, USA

Liangbing Hu

Department of Physics, University of California, Los Angeles, California 90095

Abstract

We studied the contact properties of different metals to flexible optically-transparent single-walled carbon nanotube (SWCNTs) films. The SWCNT films are deposited on flexible polyethylene terephthalate (PET) substrate and patterned in test structures optimized for contact resistance measurements for a particular metal contact. Specific contact resistance and current transfer length is determined for Pt, Cr, Cu and Au contacts. We also evaluate effects of chemical doping and thickness of SWCNT films on the contact resistance.

Many applications of flexible electronics devices such as displays, solar cells and touch screens require transparent and flexible highly-conducting electrodes. Optically transparent and electrical conductive thin films of randomly distributed carbon nanotubes have been broadly investigated as an alternative to commonly used conductive oxides [1-7]. Single-wall carbon nanotubes (SWCNT) networks demonstrate sheet resistance and optical transparency comparable to ITO on plastic substrates and, in addition, display better mechanical stability [1-7]. Characterization of contact interfaces between common metals and SWCNT films is essential for many applications. For example, to improve efficiency of solar cells, SWCNT films are often combined with metallic grids [8]. The contact resistance at the interface of the SWCNT films and metals contributes an additional resistive loss and directly affects the efficiency of the device. The trade-off between the contact area to improve the conducting properties and the resulting loss of the optical transparency has to be carefully considered. While there have been multiple investigations of transport properties of SWCNT films, sparse data are available addressing the contact resistance between metals and SWCNT films. Most of the previous research has focused on contacts to individual nanotube. [9-13]

Quantitative characterization of the contact interfaces is an interesting and challenging problem [14-17] that can be affected by multiple parameters. SWCNT films are porous materials composed of variable density of semiconductor and metal nanotubes weakly joined at numerous internal interfaces. Recent reports list wildly different specific contact resistances ranging from $2 \times 10^{-6} \Omega \text{ m}^2$ for Ag [10] to $3 \times 10^{-9} \Omega \text{ m}^2$ for Au [16] and down to $1 \times 10^{-10} \Omega \text{ m}^2$ for Pt [17] metal interfaces with nominally comparable SWCNT films.

Besides the chemical composition at the contact interfaces, the values can be affected by metal-specific three-dimensional nanoscale morphology, particular processing conditions or substrate materials.

The goal of the current paper is to compare the properties of contact interfaces between SWCNT films and typical metals fabricated under similar processing conditions relevant for the flexible electronic applications. We developed multi-layer fabrication process for patterning flexible and transparent SWCNT films on PET substrate and measured contact resistance in a well-defined geometry. A common and reliable technique, transfer length method (TLM) [18, 19], was used to determine the specific contact resistance ρ_c . We also assess the variability of the contact resistances resulting from the changes in SWCNT sheet resistance and doping level. The determined specific contact resistance and the current transfer length can provide the essential guidelines for optimization of flexible electronic devices.

The SWCNT films on flexible PET substrate were fabricated with the spraying method based on ink made of 0.8mg/mL laser ablation SWCNT in water with 1% SDBS surfactant. [20] The films were carefully rinsed in water and dried. The SWCNT film used for the measurement has resistance of 650 ohm/square and 92% transmittance at 550nm, which is typical for transparent electrodes. To prepare the test structure, we developed a multi-layer optical lithography process to pattern the SWCNT films. First, S1813 on LOR3A*, dual layer resists were spin coated on SWCNT-PET film. Then the resists were exposed by UV light through a photo-mask in a mask aligner. MF-319 was used as the developer to wash away the resists at the exposed area. Ar plasma was used to remove the exposed SWCNT film and left patterned SWCNT strips on the substrate. The residual resist was cleaned by Remover PG. Similar photolithography procedure was performed to define the metal contacts over the patterned strips. Lift-off of electron-beam deposited metal was performed in Remover PG. A typical patterned sample on PET substrate with contact leads is shown in Fig. 1(a). Fig. 1(d) and (e) are optical images of the patterned strip and metal leads of two different widths. In Fig. 1(b), we show the interface between nanotube films and metal contact layers, which illustrates good penetration of metal into SWCNT film. The distance between the contact leads S range from 10 μm to 2 mm, the strip width L and contact lead width w range from 10 μm to 200 μm . For a particular metal contact – film combination, a set of contacts is chosen to minimize the measurement error.

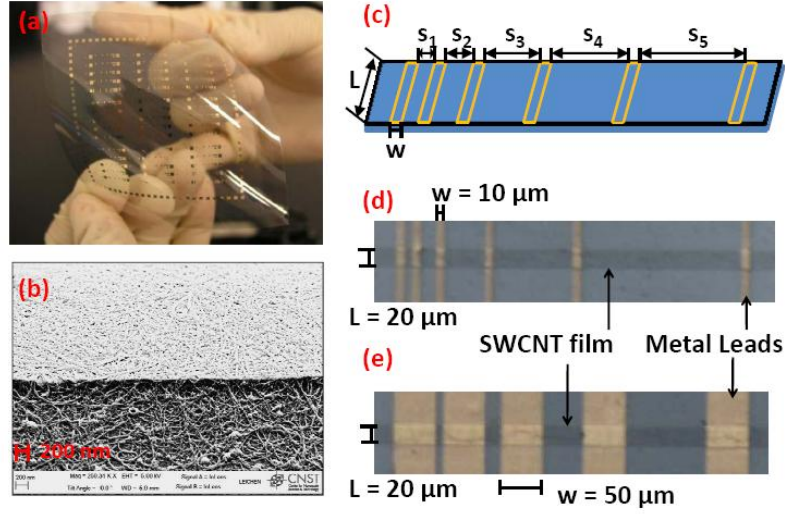


FIG. 1 (Color online) (a) Picture of the patterned sample on PET substrate (flexible and transparent) (b) SEM image of the interface between nanotube film and metal contact layer. (c) Schematic of test structure and (d) (e) the optical image of the patterned strip and metal leads.

Fig. 2(a) shows a plot of measured 2-point resistance between metal leads at different spacing. The 2-point resistance R_T can be approximately written as:

$$R_T = 2R_c + R_{sh} \frac{S_i}{L} + R_0, \quad (1)$$

where R_c is the contact resistance between the metal leads and SWCNT film, $R_{sh} \frac{S_i}{L}$ is the resistance of the SWCNT film strip, and R_0 is the serial resistance coming from the measurement cables, the resistance of metal leads itself and the contacts between cables and the metal leads. R_0 is of the order of 10^1 ohm, which is usually much less than the contact resistance and hence its contribution can be ignored.

The straight lines in Fig 2(a) are the least square fits to R_T . The intersections with the vertical axis give $2R_c$, $1.39 \pm 0.10 \times 10^4 \Omega$ and $6.60 \pm 1.0 \times 10^3 \Omega$ for $10 \mu\text{m}$ width leads with $L = 100 \mu\text{m}$ and $200 \mu\text{m}$ respectively, as illustrated in the figure. Roughly, the former contact resistance is twice of the latter one. We also measured current-voltage characteristics verifying that the contact between the metal contacts and SWCNT films is ohmic up to 1 volt.

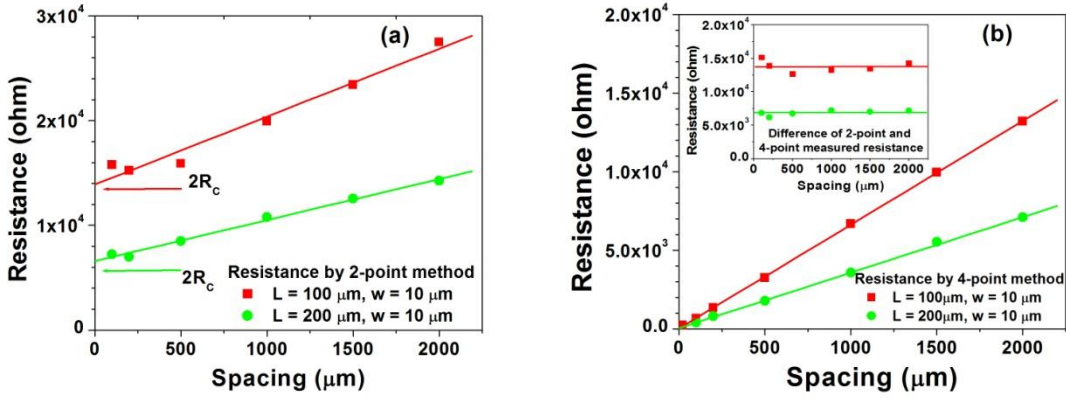


Fig. 2 (Color online) Measured resistance at different spacings for copper leads. (a) Two-point resistance as a function of leads spacing. Contact resistance R_c is determined from the intersect with Y-axis. (b) Resistance measured by 4-point method vs. lead spacing. The insert shows the difference, $2R_c$, of 2-point and 4-point resistances.

The difference between the 2-point resistance and 4-point resistance is another estimate of the contact resistance, which is shown in the insert to figure 2 (b). The averages of the differences between 2-point and 4-point measurement at different spacing, giving $2R_c$, $1.38 \pm 0.07 \times 10^4 \Omega$ and $6.60 \pm 0.30 \times 10^3 \Omega$ respectively, are consistent with the values determined from the length-dependent 2-point measurements.

The specific contact resistance ρ_c independent of contact area is an important parameter usually used to evaluate the quality of electrical contacts. For transmission line model structure, the contact resistance R_c and the specific contact resistivity ρ_c has the following relations [18, 19]:

$$\frac{R_c L}{\sqrt{R_{sh} \rho_c}} = \coth \left(w \sqrt{\frac{R_{sh}}{\rho_c}} \right), \quad \text{or} \quad \frac{R_c L}{R_{sh} L_T} = \coth \left(\frac{w}{L_T} \right) \quad (3)$$

where the characteristic transfer length $L_T = \sqrt{\frac{\rho_c}{R_{sh}}}$ defines the length over which $1/e$ of the current is transferred from metal contact to the film. Eq. 3 can be simplified as $R_c = \frac{\sqrt{\rho_c R_{sh}}}{L} = R_{sh} \left(\frac{L_T}{L} \right)$, for $w \gg L_T$ (long contact limit) or $R_c = \frac{\rho_c}{Lw}$, for $w \ll L_T$ (short contact limit). From (4), the specific contact resistivity $\rho_c = 6.7 \times 10^{-6} \Omega \cdot \text{m}^2$ is calculated.

To reduce the measurement error originating mostly from the film and the contact interface inhomogeneity, multiple two- and four-point measurements at different lead spacings and on different samples were averaged and the standard deviation was used as an error estimate.

Table 1. Specific contact resistance and transfer lengths of SWCNT films with various metal contacts.

	Pt	Cr	Cu	Au
$\rho_c (\Omega \cdot \text{m}^2)$	$5.2 \pm 1.0 \times 10^{-8}$	$2.0 \pm 0.5 \times 10^{-6}$	$6.7 \pm 2.0 \times 10^{-6}$	$5.0 \pm 2.3 \times 10^{-6}$
$L_T (\text{m})$	9.1×10^{-6}	5.5×10^{-5}	1.0×10^{-4}	8.8×10^{-5}

Besides Cu, the specific contact resistivity between SWCNT films and other metals such as Pt, Cr and Au commonly used in electrical devices was studied. The results are shown in Table. 1. We also attempted to determine the contact resistance of SWCNT films with Al and Ti. The resistance is too high possibly due to oxidation in air on PET substrate. Pt has the lowest contact resistance to SWCNT films, followed by Cr. Au and Cu display relatively high contact resistance. While the details of contact interface formation can be different for single CNT devices and CNT films, the sequence of resistances is consistent with previous studies of contact resistances to individual nanotubes [9-13]. Calculated L_T are also listed in Table. 1. For good electric contact, the lead width should be larger than L_T . We note that the range of specific contact resistances determined for different metals is much narrower than that reported in the literature for these metals [16, 17].

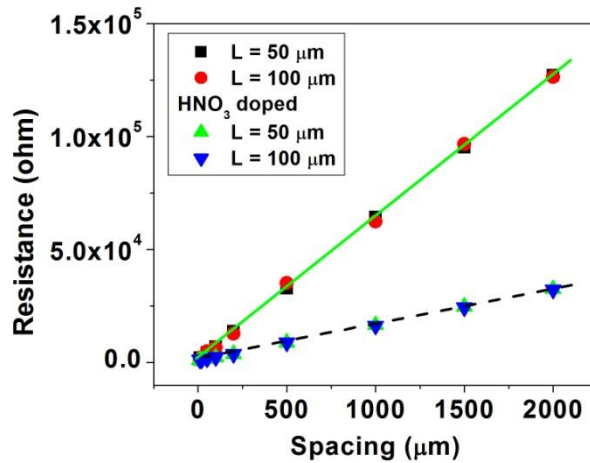


Fig. 3 Influence of the doping process on the contact resistance. Resistance measured by 2-point method for doped and undoped SWCNT films with Pt leads.

To evaluate the effect of CNT morphology and composition on the contact resistance, we use chemical doping and compare films of different thickness. Chemical doping is an effective method to improve the conductivity of SWCNT films without sacrificing optical transparency. [21, 22] The SWCNT films were doped using concentrated nitric acid (4 mol/L HNO_3). Fig. 3 shows the comparison of contact resistance measurement of SWCNT films with Pt leads with and without chemical doping. In both cases, the

determined transfer length L_T is less than half of the contact pads width ($w > 2 L_T$), and the leads are “electrically long” contacts. In this situation, the contact resistance does not depend on the leads width (see Eq. 3), which is clearly seen in Fig. 3. The results are summarized in Table. 2. While the contact resistance slightly decreases, the specific contact resistance and the transfer length actually increase for the doped film as a result of significant drop in the sheet resistance (see Eq. 3). This observation is consistent with the previous work on Ag contacts and possible microscopic explanation is suggested in [8]. The decrease of the sheet resistance is attributed to the doping and the improved conductivity of semiconductor CNTs within the film while the conductance of metal-semiconductor CNTs contacts is less affected by the doping.

Table 2. Comparison of contact resistance of undoped and doped SWCNT films with Pt leads

	R_{sh} (Ω/\square)	Transmittance @550 nm	R_c (Ω)	ρ_c ($\Omega \cdot m^2$)	L_T (m)
<i>Thin film (undoped)</i>	630	92%	575±50	$5.2 \pm 1.0 \times 10^{-8}$	9.1×10^{-6}
<i>Thin film (doped)</i>	160	92%	385±50	$9.3 \pm 2.0 \times 10^{-8}$	2.4×10^{-5}
<i>Thick film (undoped)</i>	250	85%	228±25	$1.5 \pm 0.2 \times 10^{-8}$	7.7×10^{-6}

Thicker SWCNT films can be also used to decrease the sheet resistance however the optical transmittance is adversely affected. We selected a film with 250 ohm/square sheet resistance and 85% optical transmittance at 550nm to evaluate the effect of the film thickness on the contact resistance, and the results are listed in Table 2 The thicker film has smaller contact resistance, and the specific contact resistivity roughly scales with the sheet resistance of the sample. This scaling is likely caused by the highly porous structure of the carbon nanotube films and the penetration of the evaporated metal deep through the film. This penetration can be seen in Fig.1 (a).

In summary, the contact interfaces of different metals with conductive optically-transparent SWCNT films on flexible substrate are studied and the specific contact resistance and the current transfer lengths are determined. The variation of contact resistance caused by doping and thickness of the SWCNT films is also evaluated. Pt is found to have the lowest contact resistance with SWCNT films while Au and Cu form relatively high resistance interfaces. The range of contact resistances is narrower than reported in the literature [10, 16-17] indicating that processing specific contact morphology can be as significant as the chemical composition of the contacts.

Acknowledgement

The author would like to thank the staffs of the Nanofab of the Center for Nanoscale Center for Nanoscale Science and Technology, National Institute of Standards and Technology.

Reference

1. George Gruner, *J. Mater. Chem.* **16**, 3533 (2006).
2. Z. Wu, Z. Chen, X. Du, J. M. Logan, J. Sippel, M. Nikolou, K. Kamaras, J. R. Reynolds, D. B. Tanner, F. Hebard, and A. G. Rinzler, *Science* **305**, 1273 (2004).
3. M. Zhang, S. Fang, A. A. Zakhidov, S. B. Lee, A. E. Aliev, C. D. Williams, K. R. Atkinson, and R. H. Baughman, *Science* **309**, 1215 (2005).
4. K. Bradley, J. C. P. Gabriel, and G. Grüner, *Nano Lett.* **3**, 1353 (2003).
5. D. H. Zhang, K. Ryu, X. Liu, E. Polikarpov, L. James, M. E. Tompson, and C. W. Zhou, *Nano Lett.* **6**, 1880 (2006).
6. M. W. Rowell, M. A. Topinka, M. D. McGehee, H. Prall, G. Dennler, S. Sariciftci, L. Hu, and G. Gruner, *Appl. Phys. Lett.* **88**, 233506 (2006).
7. Q. Cao, H.-S. Kim, N. Pimparkar, J.P. Kulkarni, C. Wang, M. Shim, K. Roy, M.A. Alam and J.A. Rogers, *Nature* **454**, 495-500 (2008).
8. R. Jackson and S. Graham, *Appl. Phys. Lett.* **94**, 012109 (2009).
9. J. Tersoff, *Appl. Phys. Lett.* **74**, 2122 (1999).
10. Y. Matsuda, W. Q. Deng and W. A. Goddard, *J. Phys. Chem. C* **111**, 11113, (2007).
11. F. Wakaya, K. Katayama and K. Gamo, *Microelec. Engi.* **853**, 67 (2003).
12. C. Lan, P. Srisungsitthisunti, P. B. Amama, T. S. Fisher, X. Xu and G. Reifenger, *Nanotechnology* **19**, 125703 (2008)
13. C. Lan, D. N. Zakharov and R. G. Reifenger, *Appl. Phys. Lett.* **92**, 213112 (2008).
14. A. Javey, J. Guo, Q. Wang, M. Lundstrom, and H. Dai, *Nature* **424**, 654 (2003).
15. T. Durkop, S. A. Getty, E. Cobas, and M. S. Fuhrer, *Nano Lett.* **4**, 35 (2004).
16. S. H. Han, S. H. Lee, J. H. Hur, J. Jang, Y. -B. Park, G. Irvin, and P. Drzaic, *Solid State Electronics* **54**, 586 (2010).
17. C. Koechlin, S. Maine, R. Haidar, B. Trétout, A. Loiseau, and J.-L. Pelouard, *Appl. Phys. Lett.* **96**, 103501 (2010).
18. H. H. Berger, *Solid-State Electron.* **15** 145 (1972).
19. M. Akiya and M. Aihara, *J. Phys. D: Appl. Phys.* **30**, 271 (1997).
20. L. Hu, D. S. Hecht, and G. Gruner, *Nano Lett.* **4**, 2513 (2004).
21. R. Jackson, B. Domercq, R. Jain, B. Kippelen, and S. Graham, *Adv. Func. Mater.* **18**, 2548 (2008).
22. B. B. Parekh, G. Fanchini, G. Eda, and M. Chhowalla, *Appl. Phys. Lett.* **90**, 121913 (2007).
23. * Instruments and materials are identified in this paper to describe the experiments. In no case does such identification imply recommendation or endorsement by the National Institute of Standards and Technology (NIST).